Superoxide-Generating Nox5α Is Functionally Required for the Human T-Cell Leukemia Virus Type 1-Induced Cell Transformation Phenotype

Tomonari Shigemura,[a] Masaaki Shiohara,[a] Masayoshi Kato,[b] Shuichi Furuta,[b] Kazuko Kaneda,[c] Kazuhiro Morishita,[c] Hiroo Hasegawa,[d] Masahiro Fujii,[e] Agnes Gorlach,[f] Kenichi Koike,[a] Tohru Kamata[b]

Department of Pediatrics[a] and Department of Molecular Biology and Biochemistry,[b] Shinshu University Graduate School of Medicine, Matsumoto, Nagano, Japan; Division of Tumor and Cellular Biochemistry, Faculty of Medicine, University of Miyazaki, Miyazaki, Japan[c]; Department of Laboratory Medicine, Nagasaki University Graduate School of Biomedical Sciences, Nagasaki, Japan[d]; Division of Virology, Niigata University Graduate School of Medicine and Dental Science, Niigata, Japan[e]; Experimental and Molecular Pediatric Cardiology, Department of Pediatric Cardiology and Congenital Heart Disease, German Heart Center Munich at the Technical University, Munich, Germany[f]

ABSTRACT

Human T-cell leukemia virus type 1 (HTLV-1) is associated with adult T-cell leukemia (ATL) and transforms T cells *in vitro*. To our knowledge, the functional role of reactive oxygen species (ROS)-generating NADPH oxidase 5 (Nox5) in HTLV-1 transformation remains undefined. Here, we found that Nox5α expression was upregulated in 88% of 17 ATL patient samples but not in normal peripheral blood T cells. Upregulation of the Nox5α variant was transcriptionally sustained by the constitutive Janus family tyrosine kinase (Jak)-STAT5 signaling pathway in interleukin-2 (IL-2)-independent HTLV-1-transformed cell lines, including MT1 and MT2, whereas it was transiently induced by the IL-2-triggered Jak-STAT5 axis in uninfected T cells. A Nox inhibitor, diphenylene iodonium, and antioxidants such as N-acetyl cysteine blocked proliferation of MT1 and MT2 cells. Ablation of Nox5α by small interfering RNAs abrogated ROS production, inhibited cellular activities, including proliferation, migration, and survival, and suppressed tumorigenicity in immunodeficient NOG mice. The findings suggest that Nox5α is a key molecule for redox-signal-mediated maintenance of the HTLV-1 transformation phenotype and could be a potential molecular target for therapeutic intervention in cancer development.

IMPORTANCE

HTLV-1 is the first human oncogenic retrovirus shown to be associated with ATL. Despite the extensive study over the years, the mechanism underlying HTLV-1-induced cell transformation is not fully understood. In this study, we addressed the expression and function of ROS-generating Nox family genes in HTLV-1-transformed cells. Our report provides the first evidence that the upregulated expression of Nox5α is associated with the pathological state of ATL peripheral blood mononuclear cells and that Nox5α is an integral component of the Jak-STAT5 signaling pathway in HTLV-1-transformed T cells. Nox5α-derived ROS are critically involved in the regulation of cellular activities, including proliferation, migration, survival, and tumorigenicity, in HTLV-1-transformed cells. These results indicate that Nox5α-derived ROS are functionally required for maintenance of the HTLV-1 transformation phenotype. The finding provides new insight into the redox-dependent mechanism of HTLV-1 transformation and raises an intriguing possibility that Nox5α serves as a potential molecular target to treat HTLV-1-related leukemia.

Human T-cell leukemia virus type 1 (HTLV-1) is the first human oncogenic retrovirus shown to be etiologically associated with adult T-cell leukemia (ATL) (1, 2). ATL has a poor prognosis because of its resistance to conventional chemotherapy, and no effective therapy is currently available for ATL. HTLV-1 infects and transforms human peripheral blood T cells *in vitro* (3, 4), but the precise mechanism of HTLV-1 transformation of T cells and the development of ATL after HTLV-1 infection are not fully understood. A HTLV-1 genome pX region-encoded protein, Tax, is thought to play a central role in activation, proliferation, and transformation of T cells by transactivating various cellular genes, including interleukin-2 (IL-2), IL-2 receptor α chain, and NF-κB (5–7). However, advanced ATL cells do not always express a significant amount of Tax and yet maintain the transformation phenotype (8). This raised the possibility that cellular changes, including constitutive NF-κB activation, replace Tax functions to sustain neoplastic features (8, 9). Meanwhile, IL-2 stimulates normal T-lymphocyte activity and proliferation through the Janus family tyrosine kinase (Jak)-STAT5 signaling pathway (10).

HTLV-1-infected T cells initially grow in an IL-2-dependent manner, but over time, the cells become IL-2 independent (11). In most cases, this transition seems to coincide with acquisition of constitutive activation of Jak and STAT5 signaling (12, 13), but its significance in the IL-2-independent growth mechanism remains

only partly explained. These observations suggest that, to define the functional role of HTLV-1 in malignant transformation, we need to understand more of the as-yet-unidentified sequence of intracellular signals essential for genetic and epigenetic interactions between provirus and host genes.

Accumulating evidence suggests that low levels of reactive oxygen species (ROS) act as second-messenger-like molecules in multiple cellular processes, including proliferation, apoptosis, and innate immunity. Superoxide (O_2^-)-generating NADPH oxidase (Nox) family enzymes (Nox1 to Nox5 and Duoxes 1 and 2) represent a major intracellular source for ROS (14, 15). In fact, Nox1, Nox2, and Nox4 have been shown to play important physiological and pathophysiological roles in cardiovascular, pulmonary, and renal systems. Nox1 and Nox4 may be linked to development of some types of cancers, including prostate and pancreatic cancers (16, 17). In comparison, the function of Nox5 is poorly understood. Unlike Nox1 to Nox4, Nox5 comprises the N-terminal EF hand (binding sites for calcium), in addition to the heme-containing transmembrane and NADPH/flavin adenine dinucleotide (FAD)-binding cytoplasmic domains, which are well conserved among the members of the Nox family and responsible for electron transfer from NADPH to molecular oxygen (18). There are five variants of Nox5, Nox5α, Nox5β, Nox5γ, Nox5δ, and a truncated Nox5S, depending on the splice forms of N-terminal portions (18, 19). Nox5α is present in spleen/lymph node and Nox5β in testis, while the tissue-specific distribution of Nox5γ and Nox5δ is unclear. With respect to cancer development, acid-induced Nox5S has recently been implicated in Barrett's esophageal adenocarcinoma (20). However, it is largely unknown how Nox5 functions in hematopoietic immune cells and their pathological states.

In the present study, we addressed a functional role of Nox5 in HTLV-1-transformed T cells. We found that Nox5α is a target gene of the constitutively active Jak-STAT5 cascade in IL-2-independent HTLV-1-transformed cells and that depletion of Nox5α-derived ROS impairs their ability to maintain the HTLV-1 transformation phenotype, suggesting the involvement of Nox5α in HTLV-1 pathogenesis.

MATERIALS AND METHODS

Cell lines and reagents. HTLV-1-infected T-cell lines (MT1, MT2, MT4, and HUT102) (8, 21), HTLV-1-uninfected T-cell lines (HUT78, H9, Jurkat, Molt-4, and Molt-17) (21), a HTLV-II-infected cell line (Mot) and a Bcr-Abl-positive myeloid leukemia cell line (K562) were maintained in RPMI 1640 supplemented with 10% fetal bovine serum (FBS). Diphenyleniodonium (DPI), *n*-acetyl cysteine (NAC), pyrrolidine dithiocarbamate (PDTC), AG490, STI-571 (imatinib), and STAT5 inhibitor were purchased from Calbiochem. Rabbit anti-Nox5 antibodies were produced as described previously (22) or purchased from Novus Biologicals. Antibodies against phospho-AKT (Thr308), AKT, phospho-extracellular signal-regulated kinase (ERK) (Thr202/Tyr204), ERK, STAT5, and phospho-STAT5 (Tyr694) were purchased from Cell Signaling. pGD210-Bcr-Abl was provided by T. Tauchi and pcDNA3.1-myc-STAT5B-CA by K. Ikuta.

Human specimens. The study protocol was approved by the Human Ethics Review Committee of Shinshu University, and all samples were collected after obtaining informed consent from patients. Peripheral blood mononuclear cells (PBMC) from healthy volunteers and ATL patients were purified by Ficoll-Hypaque gradient centrifugation (Amersham Bioscience) as described previously (8).

Construction of siRNA and reporter plasmids. Duplex, small interfering RNA (siRNA) oligonucleotides for human Nox5 and a nonspecific control were subcloned into the pSilencer 5.1-HI Retro vector (Ambion) according to the manufacturer's instructions. siRNAs were designed as follows: 5′-GATCCACTCAAATTCCTCTTCCAGTTCAAGAGACTGG AAGAGGAATTTGAGTTTTTTTGGAAA-3′ for siNox5α and 5′-GATC CGCTCCATAAGGTGGACTTTTTCAAGAGAAAAGTCCACCTTATG GAGCTTTTTTGGAAA-3′ for siNox5α-I. pGL3-Nox5 was constructed as follows: the fragment (−1502 to −11 from ATG in exon 3) of human Nox5 gene which encompasses two putative STAT binding sequences of TTCCCTTAA (−1380 to −1382 and −733 to −725) was PCR amplified from HeLa cell genomic DNA and subcloned into pGL3basic (Promega) at HindIII sites.

Transfection and immunoblotting. Cells were transfected with the indicated vectors or siRNAs utilizing Lipofectamine 2000 (Invitrogen) according to the manufacturer's protocol. Cell lysates were prepared in radioimmunoprecipitation assay (RIPA) buffer, and immunoblotting analysis was performed using appropriate antibodies as described previously (23).

Isolation of stable transfectants. Packaging cells were transfected with pSilencer 5.1-HI Retro vector carrying siNox5α or scrambled siRNAs by using FuGene6 (Roche). The culture supernatant containing viruses was harvested 72 h after transfection. MT1 and MT2 cells were infected with retroviruses according to the manufacturer's instructions and subjected to selection with 350 µg/ml puromycin. Cloned cell lines were maintained with 5 µg/ml puromycin.

Promoter activity assay. Jurkat T cells (4×10^5) were transfected with pGL3-Nox5α (0.4 µg) and pGD210-Bcr-Abl (0.4 µg) and treated with STAT5 inhibitor (Calbiochem) for 24 h. Alternatively, MT1 and MT2 cells were transfected with pGL3-Nox5α (0.4 µg) together with scrambled or STAT5B siRNAs (Invitrogen). Cells were lysed, and lysates were subjected to promoter activity assay with a reporter assay kit (Promega) according to the manufacturer's protocol.

Cell growth assay. Cells were grown in the presence or absence of antioxidants and DPI, and live cells were counted.

Measurement of ROS production. Cells were inoculated into 96-well plates and incubated with 200 µM luminol and 1 U of horseradish peroxidase in Hanks balanced salt solution (HBSS) for 20 min at 37°C as described previously (24). Luminescence was quantified by the use of a Lumat LB9507 Luminometer (Berthold).

Annexin V-PE assay. The annexin V-phycoerythrin (PE) assay (BD Biosciences) was performed according to the manufacturer's instructions. Briefly, cells were collected and stained with annexin V or Via probe. Cell surface markers were analyzed with a FACScan flow cytometer, using the software program BD FACStation-Data Management System (BD Biosciences). Fractions of annexin V-positive cells were estimated.

RT-PCR and real-time PCR. Reverse transcription (RT) was performed by the use of a ReverTra Ace kit (Toyobo). Real-time PCR was performed with the specific primers (available upon request) for detection of Nox5 by using TaqMan gene expression (assay Hs00225846_m1; Applied Biosystems) (see Fig. 4B) or for detection of Nox isoforms by using the Mesa green quantitative PCR (qPCR) MasterMix Plus for SYBR assay protocol (Eurogentec) (see Fig. 2). The data were normalized to the expression levels of β-actin and calculated by the threshold cycle ($\Delta\Delta C_T$) method.

Cell migration assay. Cells were seeded in serum-free media into the top of a Boyden chamber (BD Bioscience). Media containing 5% FBS were added to the bottom of the chamber. After 24 h of incubation, the migrated cells were stained with crystal violet and counted according to the manufacturer's protocol.

Tumorigenicity assay. NOG mice were obtained from the Central Institute for Experimental Animals (Kawasaki, Japan). Cells (4×10^7) were suspended in phosphate-buffered saline (PBS) and subcutaneously injected into mice (6 mice for one group) as described previously (25). Mice were sacrificed during the 4-to-5-week follow-up period after inoculation. Tumors were measured with an external caliper, and volume was calculated as described previously (26).
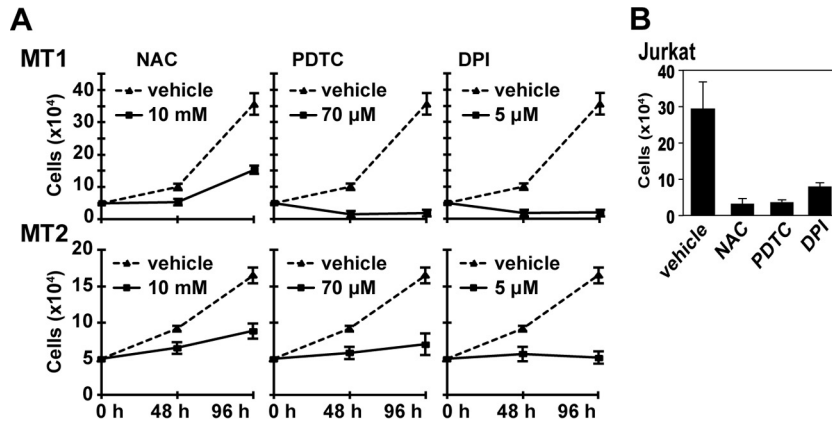
FIG 1 Effects of antioxidants and DPI on proliferation of HTLV-1-infected MT1 and MT2 cells. (A) MT1 and MT2 cells (5×10^4) were cultured in the presence or absence of the indicated amounts of NAC, PDTC, and DPI. The cell growth was determined at the indicated time intervals. The data represent means ± standard deviations (SD) ($n = 3$) of the results from four separate experiments. (B) Jurkat T cells (5×10^4) were cultured in the presence of DPI (0.5 μM), PDTC (14 μM), NAC (2 mM), or dimethyl sulfoxide (DMSO) for 48 h, and the cells were counted. The data represent means ± SD ($n = 3$) of the results from three separate experiments. For the data presented throughout panels A and B, statistical analysis was performed with one-way ANOVA, followed by Dunnett's multiple-comparison t test. P value for comparisons of chemical treatment versus vehicle, <0.05.

Immunohistochemistry. Tumor tissues were fixed, and tissue sections were embedded in paraffin and subjected to antigen retrieval in a microwave in Tris-HCl-EDTA buffer (pH 8.0) as described previously (27). Sections were incubated with anti-CD4 and anti-CD25 antibodies (Thermo Fisher Scientific) and subsequently with horseradish peroxidase (HRP)-conjugated secondary antibodies and were counterstained with hematoxylin. 3,3′-Diaminobenzidine was used as a chromogen.

Statistical analysis. Data represent the means ± standard deviations of results from at least three separate experiments. Statistical analysis of the results from the two groups was performed using Student's t test. One-way analysis of variance (ANOVA) was performed with two or more groups, followed by Dunnett's multiple-comparison test or the Bonferroni test. Differences with P values of <0.05 were considered to be statistically significant. All statistical analyses were performed with IBM SPSS version 22 software.

RESULTS

ROS production is required for growth of HTLV-1-infected cells. To understand the role of ROS-generating machinery in HTLV-1-infected T cells, we first examined whether ROS generation is required for the growth of two HTLV-1-infected T-cell lines, MT1 and MT2. DPI, a general inhibitor for Nox enzymes and antioxidants, NAC, and PDTC decreased the growth rate of cells (Fig. 1A). To achieve a similar level of inhibition, much lower concentrations of these agents were required for uninfected Jurkat T cells (Fig. 1B). This suggests that Nox family genes are involved in ROS-mediated growth control of MT1 and MT2 cells.

To further explore the nature of the Nox isozymes involved, the expression of Nox family mRNAs was examined. Real-time PCR analysis revealed that Nox5 but not other Nox family members was expressed in HTLV-1-infected cell lines, namely, MT1, MT2, MT4, and HUT102 (Fig. 2A). In contrast, the Nox5 transcripts were not expressed in HTLV-1-uninfected T-cell lines (Fig. 2A) or in normal peripheral blood T cells (Fig. 2B). Notably, the levels of Nox5 mRNAs were elevated in 15 of 17 PBMC samples freshly isolated from ATL patients compared with those in normal controls (Fig. 2B and Table 1). No significant correlation was found between expression of other Nox isoforms and HTLV-1 infection/ATL pathogenesis (Fig. 2A and C). Thus, it is most likely

that Nox5 is specifically upregulated in both HTLV-1-transformed cell lines and a subset of primary ATL cells.

The Nox5α variant is expressed in MT1 and MT2 cells. Previous reports described five Nox5 variants—those (α, β, γ, and δ) that differ in the sequence of the N-terminal calcium-binding domains and a spliced short variant (Nox5S) lacking this domain (18, 19). We therefore determined which of the Nox5 variants exists in MT1 and MT2 cells. RT-PCR together with DNA sequencing showed that a primer set (primers a/b) generated a 433-bp fragment encompassing the region between exon 13 and exon 17 common to Nox5L and Nox5S, whereas another primer set (primers c/d) generated a 536-bp fragment which corresponds to the region between exon 3 and exon 6 of Nox5α but not to that of Nox5γ, with an extra 84-bp insertion (Fig. 3A and B). Moreover, a primer set (primers d/e) specific to Nox5β and Nox5δ generated no DNA fragment, indicating that Nox5β, Nox5γ, and Nox5δ were not expressed. The data suggest that Nox5α was expressed but do not exclude the possibility of the presence of Nox5S. Immunoblotting with antibodies against the COOH-end region of Nox5 detected 75-kDa Nox5α but not the 60-kDa Nox5S short variant in the cell lysates. Together, the data confirmed that the Nox5 variant in MT1 and MT2 cells is Nox5α (Fig. 3C).

Nox5α siRNAs suppress ROS production in MT1 and MT2 cells. We next examined whether Nox5α-derived ROS are required for proliferation of MT1 and MT2 cells. To this end, two siRNAs for Nox5α were tested for knockdown efficiency. Immunoblotting analysis with anti-Nox5α antibodies showed that loading with siNox5α decreased the expression of Nox5α proteins more efficiently than loading with siNox5α-I in MT2 cells (Fig. 4A). We therefore used siNox5α to disrupt endogenous Nox5α in the subsequent experiment. Real-time PCR and immunoblotting demonstrated that the amounts of both Nox5α mRNAs and Nox5α proteins were decreased in Nox5α siRNA-transfected MT1 and MT2 cells (MT1siNox5 and MT2siNox5 cells) compared with those in scrambled siRNA-transfected cells (MT1SC and MT2SC cells) (Fig. 4B and C), which indicates
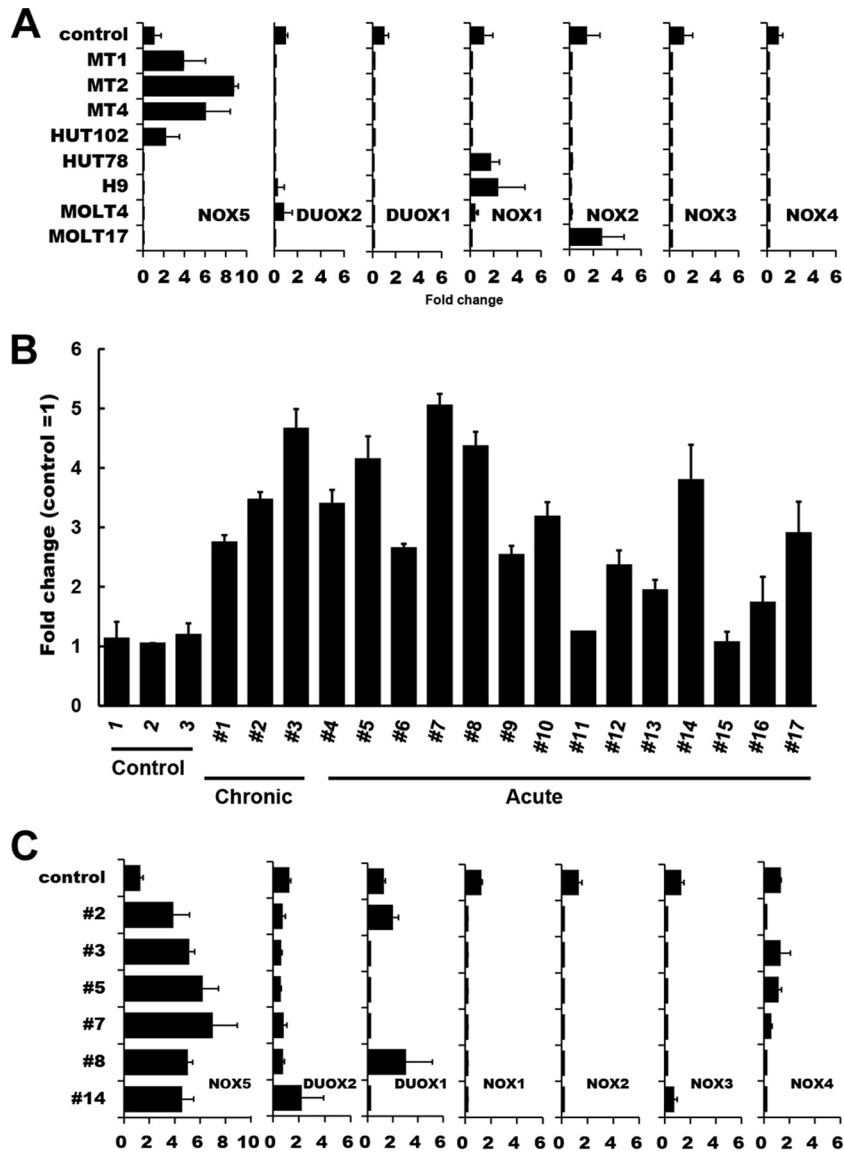
FIG 2 Analysis of Nox family expression in HTLV-1-infected T-cell lines and ATL PBMC. (A) Total RNAs were extracted from various HTLV-1-infected (MT1, MT2, MT4, and HUT102) and HTLV-1-uninfected (HUT78, H9, MOLT4, and MOLT17) T cells, and levels of mRNA expression of Nox family members were analyzed by real-time PCR. Control data represent normal T cells. One-way ANOVA was performed to determine differences between HTLV-1-infected and -uninfected cell lines. There was a statistically significant difference only in the Nox5 expression data ($P < 0.05$ versus control). (B) The levels of Nox5 mRNA expression in ATL primary cells (Table 1) were examined by real-time PCR. CTL (control), normal PBMC. The data represent means ± SD ($n = 3$) of results from three separate experiments. (C) Comparison of levels of Nox isoform expression in ATL patient samples. A total of 6 samples were randomly selected from 17 ATL patient samples which had been analyzed as described for panel B and subjected to the analysis of Nox isoform expression by real-time PCR. Control, normal PBMC. β-Actin was used as an internal control. The data represent means ± SD ($n = 3$) of results from three separate experiments. Note that, among the Nox family members, only the levels of Nox5 were increased in the 6 ATL patient samples examined.

that Nox5α siRNAs eliminate the Nox5α transcript from the cells. Then, the effects of Nox5α siRNAs on intracellular production of hydrogen peroxide were examined by a luminol assay. Catalase-inhibitable ROS generation was significantly attenuated in MT1siNox5α cells and MT2siNox5α cells compared with control cells (Fig. 4D), suggesting the involvement of Nox5α in ROS synthesis in HTLV1-infected cells. In control experiments, Nox5α siRNAs did not suppress ROS production in uninfected H9 cells (data not shown).

Effects of Nox5α siRNAs on both proliferation and cell survival of MT1 and MT2 cells. Since growth of MT1 and MT2 cells

was inhibited by DPI, NAC, and PDTC (Fig. 1), we investigated whether the suppression of Nox5α with Nox5α siRNAs blocks cell proliferation. Both growth in liquid culture (Fig. 5A) and colony formation (Fig. 5B) of MT1siNox5α and MT2siNox5α cells were significantly reduced compared with those of MT1SC and MT2SC cells, respectively. Immunoblotting with anti-phospho-ERK antibodies indicated that the activated, phosphorylated form of ERK, a key growth signal transducer, was diminished by knockdown of Nox5α (Fig. 4C). Neither cell growth nor Erk/Akt activity was affected in uninfected H9 cells upon transfection of Nox5α siRNAs (data not shown). These results

TABLE 1 Clinical characteristics of ATL patients[a]

Patient	Disease type	No. of WBC ($\times 10^3/\mu l$)	Atypical lymphocytes (%)
1	Chronic	15.5	45
2	Chronic	11.9	41
3	Chronic	15.8	65
4	Acute	7.5	ND
5	Acute	41.8	87
6	Acute	15.7	24
7	Acute	26.8	86
8	Acute	8.3	ND
9	Acute	194.5	ND
10	Acute	17.9	20
11	Acute	21.2	49
12	Acute	30.0	56
13	Acute	ND	ND
14	Acute	ND	ND
15	Acute	65.6	66
16	Acute	17.8	54
17	Acute	117.2	57

[a] WBC, white blood cells; ND, not determined.

suggest that Nox5α-derived ROS, at least in part, sustain proliferation of MT1 and MT2 cells.

Inhibition of cell proliferation is frequently associated with induction of apoptosis. We therefore explored whether ablation of Nox5α with Nox5α siRNAs leads to cell death. Annexin V labeling demonstrated that transfection of Nox5α siRNAs into MT1 and MT2 cells increased apoptosis induction compared with that of scrambled controls when the transfected cells were serum starved (Fig. 5C) or treated with a chemotherapeutic agent, adriamycin (Fig. 5D). Furthermore, silencing of the Nox5α activity reduced phosphorylation of AKT, a major cell survival signal mediator (Fig. 4C). These data suggest that Nox5α endows MT1 and MT2 cells with the cell survival activity and that ablation of Nox5α sensitizes the cells to proapoptotic agents. From the therapeutic viewpoint, it is noteworthy that inactivation of Nox5α enhances the efficacy of adriamycin.

Inhibition of Nox5α suppresses cell migration. We next examined the effects of Nox5α inhibition on the migratory activity of MT1 and MT2 cells. A migration assay demonstrated that the numbers of migrating cells were markedly reduced in MT1siNox5α and MT2siNox5α cells (Fig. 5E), implying that Nox5α contributes to motility of HTLV-1-transformed cells.

Nox5α expression is regulated by the Jak-STAT5 pathway. It remains to be determined how the Nox5α activity is regulated in the HTLV-1-transformed cells. Although the Tax viral transactivator is known to affect numerous cell cycle progression genes (28), it seems unlikely that Tax regulates Nox5α expression because we failed to detect induction of Nox5α expression following overexpression of Tax (data not shown). Given that Jak1 and Jak3 and their phosphorylation targets, STAT5A and STAT5B, are constitutively activated in HTLV-1-transformed cells, thereby controlling cellular proliferation (12, 13), we assumed that the Jak-STAT5 pathway might be coupled to the Nox5α signaling. RT-PCR analysis showed that treatment of MT1 and MT2 cells with a Jak inhibitor, AG490, decreased the level of Nox5α mRNAs (Fig. 6A). Similarly, transfection of STAT5B siRNAs blocked constitutive expression of Nox5α (Fig. 6C). Immunoblotting analysis performed with anti-phospho-STAT5B antibodies confirmed

that elevated tyrosine phosphorylation of STAT5B was blocked by treatment with AG490 (Fig. 6E). Moreover, Nox5α was not upregulated in an HTLV-II-infected cell line, Mot, in which the Jak/STAT pathway is not activated (29) (Fig. 6G). Thus, constitutive activation of the Jak-STAT5 axis seems to sustain the expression of Nox5α in HTLV-1-transformed cells.

The Jak-STAT5 pathway also plays a pivotal mediating role in the IL-2 signaling involved in the growth and survival of T cells, where ligation of IL-2 to IL-2 receptor β and γ chains results in activation and recruitment of Jak1 and Jak3 and phosphorylation and nuclear translocation of STAT5A and STAT5B (30). We therefore addressed the activation of Nox5α upon stimulation of the IL-2 signaling pathway. IL-2 treatment induced expression of Nox5α in Jurkat T cells, whereas both addition of AG490 and transfection of STAT5B siRNAs suppressed induction of Nox5α expression by IL-2 (Fig. 6B and D). Treatment with IL-2 or phorbol myristate acetate/phytohemagglutinin (PMA/PHA), which involves Jak/STAT5, also induced Nox5α expression in normal PBMC (Fig. 6H). The data implied that the activated Jak-STAT5 pathway targets the Nox5α gene in response to IL-2 stimulation. Because STAT5 is constitutively phosphorylated and activated by Bcr-Abl tyrosine kinase oncogene, the product of the t (9:22) (q34: q11) translocation in chronic myelogenous leukemia (CML) cells (31), the expression level of Nox5α was examined in a CML cell line, K562. Nox5α expression was spontaneously upregulated,
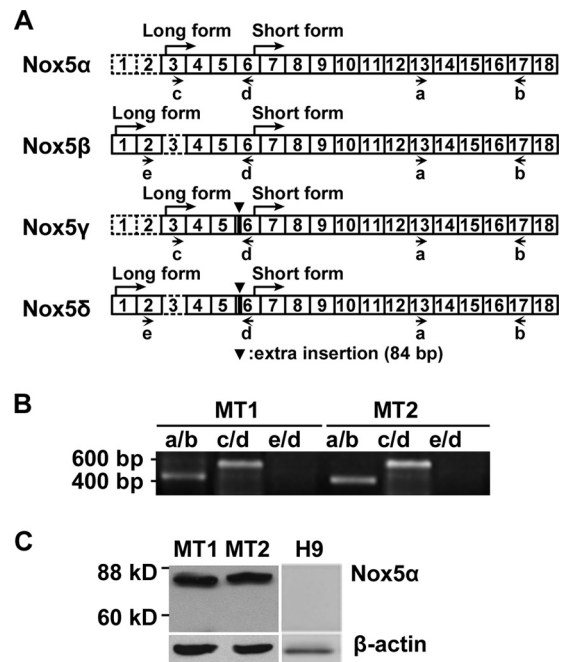

FIG 3 Identification of Nox5α variants in MT1 and MT2 cells. (A) A schematic figure shows the configuration of exons in four Nox5 splice variants (α, β, γ, and δ) belonging to an L-form and in Nox5S, a short form lacking an N-terminal calmodulin-like Ca^{2+} binding domain. The exons were numbered based on GenBank sequences as follows: α, AF353088; β, AF325189; γ, AF353089; δ, AF325190. Letters a to e indicate the positions of primers used for PCR analysis as described for panel B. (B) Levels of mRNA expression of Nox5 variants in MT1 and MT2 cells were analyzed by RT-PCR. Primers a, b, c, d, and e were assigned as shown in Fig. 3A. PCR products were analyzed by sequencing. (C) Lysates from MT1, MT2, and H9 cells were prepared and subjected to immunoblotting with antibodies against the COOH-end peptide of Nox5. β-Actin was used as a loading control.
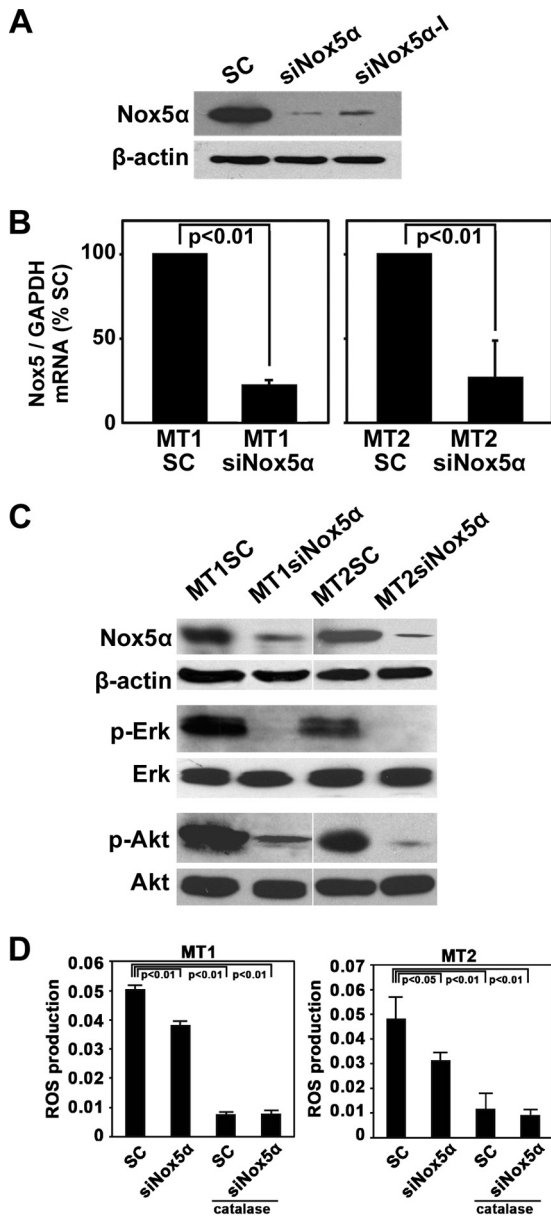
FIG 4 Nox5α siRNA reduces both phosphorylation of Erk and AKT and ROS production. (A) Lysates were prepared from MT2 cells transfected with scrambled siRNA (SC) or a Nox5-specific siRNA (siNox5α or siNox5α-I) and were subjected to immunoblotting with anti-Nox5 or anti-β-actin antibodies. (B) MT1 and MT2 cell lines stably transfected with Nox5α siRNA (MT1siNox5α and MT2siNox5α) or scrambled siRNA (MT1SC and MT2SC) were established. Expression levels of Nox5α mRNAs were examined by real-time PCR using GAPDH (glyceraldehyde-3-phosphate dehydrogenase) as an internal control. The data represent means ± SD ($n = 3$) of results from three separate experiments. Student's t test was performed. (C) Expression levels of endogenous Nox5α proteins in the indicated cell lines were determined by immunoblotting with anti-Nox5 antibodies. β-Actin was used as a loading control. Alternatively, phosphorylation levels of Erk and AKT were examined by immunoblotting with anti-phospho-Erk and anti-phospho-AKT antibodies. (D) Levels of intracellular ROS in MT1siNox5α, MT1SC, MT2siNox5α, and MT2SC cells were measured by luminol assay in the presence or absence of catalase (250 U/ml). The data represent means ± SD ($n = 4$) of results from three separate experiments. Statistical analysis was performed with ANOVA, followed by the Bonferroni test.

and this expression was blocked by an Abl-specific tyrosine kinase inhibitor, STI-571, and, to a lesser extent, by AG490 (Fig. 6A). STAT5B siRNAs also abrogated Nox5α mRNAs (Fig. 6C). Furthermore, increased STAT5B phosphorylation was attenuated upon treatment with AG490 (Fig. 6E) and STI-571 (Fig. 6F). The data suggest that Nox5α expression is also upregulated by Bcr-Ab1 through phosphorylation of STAT5B in CML cells.

Transcriptional activation of the Nox5α promoter by STAT5. To further assess the transcriptional regulation of Nox5α by STAT5, we created a luciferase reporter construct carrying the −1502 to −11 (positions from ATG) region of the Nox5α promoter, which contains two consensus STAT5 biding sequences (Fig. 7A). We found that STAT5B siRNAs markedly reduced the Nox5α promoter activity in both MT1 and MT2 cells (Fig. 7B), indicating that STAT5B induces the activation of the Nox5α promoter. The Nox5α promoter activity was enhanced following overexpression of Bcr-Abl in Jurkat T cells, whereas this enhancement was diminished by treatment with a STAT5 inhibitor (Fig. 7C). Furthermore, transfection of a constitutively active STAT5B-CA mutant (32) enhanced the Nox5α promoter activity (Fig. 7D). This suggests that STAT5 mediates Bcr-Abl-induced activation of the Nox5α promoter, but we do not formally rule out the possibility that STA5B binds to other sites distinct from the predicted regions.

Nox5α siRNAs suppress tumor formation by HTLV-1-transformed cells. To address the contribution of Nox5α to HTLV-1-induced tumorigenesis, we tested whether HTLV-1-transformed cells become less tumorigenic due to overexpression of Nox5α siRNAs in a mouse xenograft assay. Scrambled siRNA- and Nox5α siRNA-transfected MT2 cell lines were inoculated subcutaneously into NOG mice. The animals have been used for successful engraftment of HTLV-1-transformed human T cells (33). While scrambled siRNA-transfected cells produced a visible tumor within a 4-week period, expression of Nox5α siRNAs resulted in a marked decrease in the tumor growth rate (Fig. 8). Both a leukemia-expressing T-cell marker, CD4, and an activating marker, CD25 (IL-2Rα), were expressed in the tumor cells (Fig. 8). Thus, Nox5α siRNAs inhibit the tumorigenicity of MT2 cells, suggesting an important mediating role of Nox5α-derived ROS in HTLV-1-dependent transformation.

DISCUSSION

HTLV-1 is the causative agent of ATL, a CD4$^+$ T-cell-specific leukemia. The precise mechanism of the neoplastic growth of HTLV-1-transformed T cells currently remains unclear. In the present study, we demonstrated that Nox5α expression is upregulated in HTLV-1-transformed cell lines. Augmented Nox5α-generated ROS are required for proliferation, migration, and survival of HTLV-1-transformed cells, with accompanying ERK and AKT phosphorylation cascades. Furthermore, ROS generation by Nox5α contributes to formation of tumors derived from HTLV-1-transformed cells in NOG mice. To our knowledge, this is the first evidence that Nox5α-derived ROS play a critical biological role in maintenance of the HTLV-1 transformation phenotype. Identification and characterization of a putative sensor for Nox5α-generated ROS, which would be crucial in understanding the Nox5α action, have to await future investigation.

Another major finding is that the Nox5α promoter contains STAT5 transcription factor binding sequences and that inhibition of the STAT5 activity by either a Jak inhibitor or STAT5B siRNAs suppresses Nox5α mRNA synthesis as well as Nox5α promoter
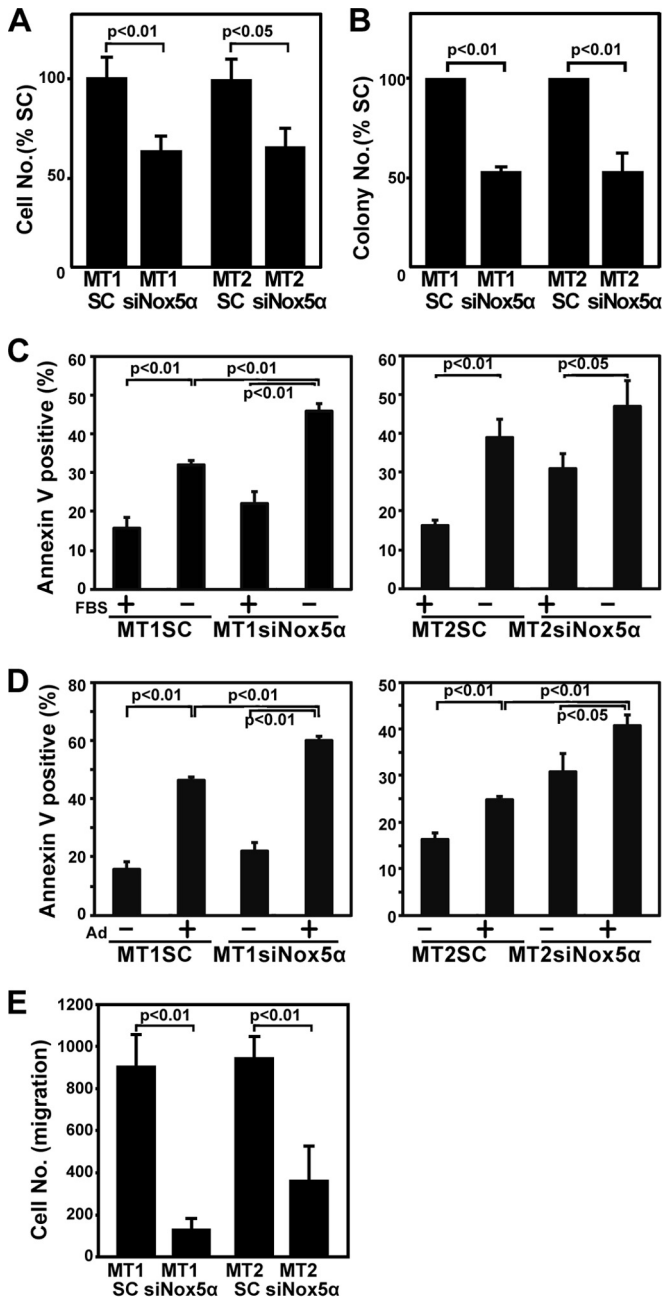
FIG 5 Inhibition of Nox5 suppresses proliferation, cell survival, and migration of MT1 and MT2 cells. (A) Growth rates of indicated cell lines in liquid culture. Cells (5×10^3) were plated, and the numbers of live cells were determined 48 h later. The cell numbers of MT1SC and MT2SC at 48 h were 1.5×10^4 and 1.0×10^4, respectively. The data represent means ± SD ($n = 3$) of results from three separate experiments. Student's t test was performed. (B) Cells (5×10^3) were inoculated into 6-well plates in 1 ml of MethoCult (H4230; Stemcell Technologies, Tukwila, WA) containing 10% FBS. Colonies were counted 10 days later. The data represent means ± SD ($n = 3$) of results from three separate experiments. Student's t test was performed. (C and D) MT1SC, MT1siNox5α, MT2SC, and MT2siNox5α cells were serum (FBS) starved for 48 h (C) or treated with 4 μM adriamycin (Ad) for 48 h (D) using the indicated combinations and subjected to an annexin V-apoptosis assay. The data represent means ± SD ($n = 3$) of results from four separate experiments. One-way ANOVA was performed, followed by the Bonferroni test. (E) Cells were plated and subjected to a cell migration assay as described in Materials and Methods. The data represent means ± SD ($n = 4$) of results from three separate experiments. Student's t test was performed.
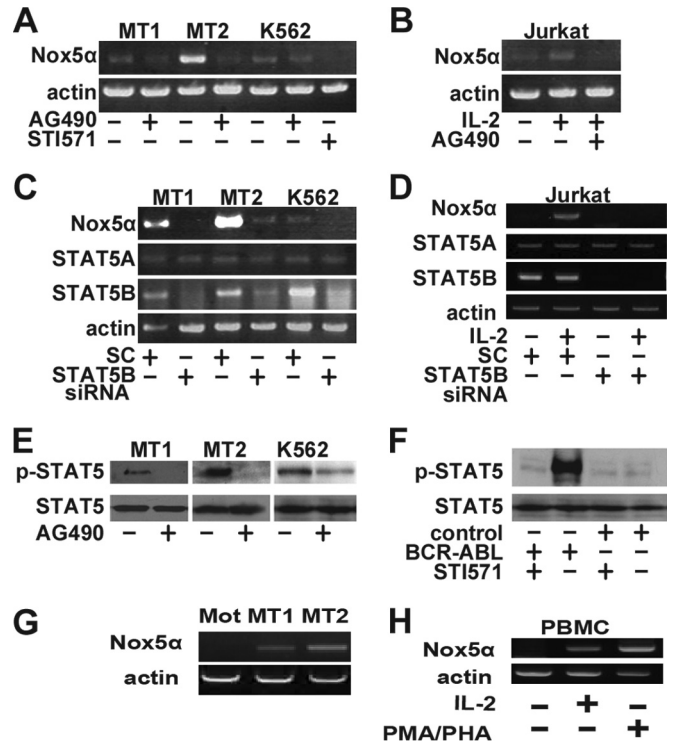

FIG 6 Nox5α expression is blocked by inhibition of Jak, BCR-Ab1, and STAT5. (A) MT1, MT2, and K562 cells were treated with 50 μM AG490 (Jak inhibitor) or 250 nM STI-571 (BCR-Ab1 inhibitor) for 24 h, and levels of Nox5α expression were examined by RT-PCR. (B) Jurkat T cells were treated with IL-2 (100 ng/ml) in the presence or absence of 50 μM AG490 for 24 h, and Nox5α expression was examined by RT-PCR. (C) MT1, MT2, and K562 cells were transfected with STAT5B siRNA or scrambled siRNA, and the levels of expression of Nox5α, STAT5A, and STAT5B were examined by RT-PCR. (D) Jurkat T cells were transfected with STAT5B siRNAs or with scrambled siRNA and stimulated with IL-2 (100 ng/ml) for 24 h or left unstimulated. The levels of expression of Nox5α, STAT5A, and STAT5B were examined by RT-PCR. In the experiments whose results are shown throughout panels A to D, β-actin was used as an internal control. (E and F) MT1, MT2, and K562 cells were treated with 50 μM AG490 for 24 h (E); alternatively, HEK293 cells were transfected with Bcr-Abl or control vector and treated with 250 nM STI-571 for 24 h (F). Lysates were subjected to immunoblotting with anti-phospho-STAT5 (Tyr694) and anti-STAT5 antibodies. (G) Nox5α is not upregulated in HTLV-II-infected T cells. The levels of Nox5α expression in Mot (HTLV-II-infected T cell line), MT1, and MT2 cells were examined by RT-PCR. (H) Nox5α expression is induced in IL-2- or PHA/PMA-stimulated PBMC. PBMC were treated with IL-2 (100 ng/ml) or PHA (100 ng/ml)/PMA (5 μg/ml) for 24 h and subjected to RT-PCR analysis of Nox5α expression. β-Actin was used as an internal control in the experiments whose results are shown in panels G and H.

activity in MT1 and MT2 cells. HTLV-1-transformed cells exhibit constitutive tyrosine phosphorylation of Jak3 and STAT5 (12, 13), and lymphocytes isolated from HTLV-1-infected patients display tyrosine phosphorylation of Jak3, STAT3, and STAT5 (34, 35). STAT proteins are activated in many human cancers and serve as oncoproteins by promoting cell proliferation (36). These observations suggest that sustained expression of Nox5α is induced as a consequence of constitutive activation of the STAT5 transcriptional activity by Jak in HTLV-1-transformed cells, contributing to their growth. Meanwhile, the Jak-STAT5 pathway serves as the major IL-2 downstream signaling pathway controlling T-lymphocyte function, including cell proliferation (10). Our data indicate
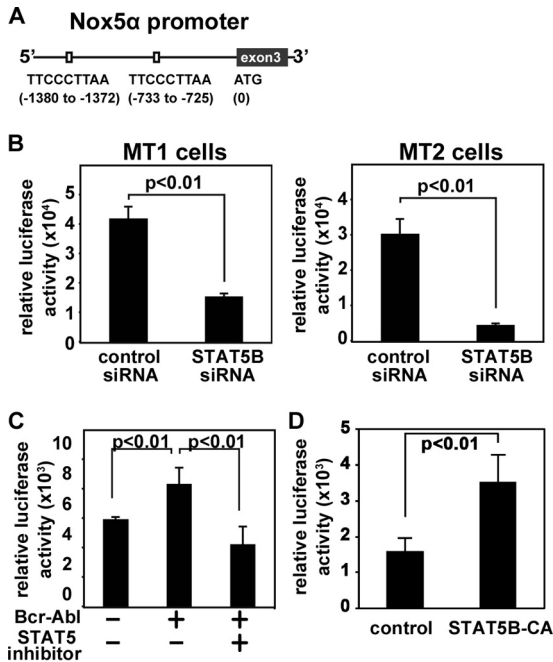
FIG 7 Activation of Nox5α promoter activity through STAT5. (A) Schematic structure of the 5′-flanking region of the Nox5α promoter. The consensus STAT5-binding sites (TTCCCTTAA) are shown in the Nox5α promoter region (-1502 to -11 from ATG in exon 3) subcloned into pGL3basic. (B) MT1 and MT2 cells were transfected with pGL3-Nox5α (-1502 to -11) together with STAT5B siRNAs or control siRNAs. Lysates were subjected to a reporter assay. The data represent means ± SD ($n = 3$) of results from three separate experiments. Student's t test was performed. (C) Jurkat T cells were transfected with pGL3-Nox5α (-1502 to -11) together with pGD210-Bcr-Ab1 or control vectors and treated with STAT5 inhibitor (250 nM) for 24 h. Lysates were subjected to a reporter assay. The data represent means ± SD ($n = 3$) of results from three separate experiments. One-way ANOVA was performed, followed by the Bonferroni test. (D) Jurkat T cells were cotransfected with pGL3-Nox5α (-1502 to -11) together with the STAT5B-CA mutant or control vector and subjected to a reporter assay. The data represent means ± SD ($n = 3$) of results from three separate experiments. Statistical analysis was performed with Student's t test.

that IL-2 transiently induced expression of Nox5α in a Jak-STAT5-dependent manner in non-HTLV1-transformed T cells, which contrasts with the result of constitutive Nox5α expression in IL-2-independent MT1 and MT2 cells. Thus, we speculate that Nox5α functions as an integral component of Jak-STAT5-mediated IL-2 signaling under normal circumstances and that HTLV-1 activates Nox5α by overriding the constitutive Jak-STAT5 signal-

ing pathway. Although the modulation by the Tax HTLV-1 trans-activator of the expression of various genes in HTLV-1-transformed cells is well documented (7), Tax does not seem to regulate Nox5α expression, because overexpression of exogenous Tax failed to induce Nox5α (data not shown). p12^I, the gene product of the HTLV-1 pX region, has been suggested to be an activator of STAT5 (37). However, overexpression of p12^I in Jurkat T cells did not activate the Nox5α promoter activity (data not shown), which makes it unlikely that p12^I controls the transcription of Nox5α. Further study is required for identification of a HTLV-1 protein(s) responsible for triggering the Jak-STAT5-Nox5α axis.

Our study also showed that Nox5α was expressed in 88% of 17 ATL patients' PBMC samples, whereas no Nox5α was detected in that of the health counterparts. This high incidence indicates that Nox5α is expressed not only in HTLV-1-infected cell lines but also in primary ATL cells. The finding suggests some correlation of Nox5α expression with ATL development, although it is obviously necessary to study many more cases.

Examining the involvement of Nox5α in other hematopoietic neoplasms, we found that Nox5α is also upregulated in Bcr-Ab1-positive CML cells but not Bcr-Abl-negative HL-60 cells (data not shown) and that Nox5α expression is induced by the Bcr-Ab1 tyrosine kinase oncogene through phosphorylation of STAT5. Thus, Nox5α participates in the bioactivity of CML as well as that of HTLV-1-transformed T cells, indicating its wide-ranging roles in hematologic malignancy. Nox5 was also suggested to be involved in hairy cell leukemia, a chronic B-cell malignancy (38).

ROS have been implicated in the regulation of some biological activities in HTLV-1-infected cells. For example, expression of ATL-derived factor (ADF), a homologue of thioredoxin (TRX), is enhanced in HTLV-1-infected cells, and ADF appears to be involved in their autocrine growth (39, 40). ADF seems to transmit signals by regulating ASK1 via a redox reaction. Since the interaction of TRX-ASK1 is not affected by Nox isozyme-derived ROS (41), it is unlikely that Nox5α participates in the ADF/ASK1 pathway. p13, a HTLV-1-encoded protein located in mitochondria, also increases ROS generation and thereby induces the death of HTLV-1-infected cells, contributing to the turnover between normal and HTLV-1-transformed cells (42). However, Nox-dependent ROS generation is not affected by the mitochondrial oxidase inhibitor rotenone and appears to be functionally different from mitochondrial ROS production (14). Thus, the current study has significance in the sense that it revealed the alternative impact of ROS signaling with respect to the biology of HTLV-1 infection.

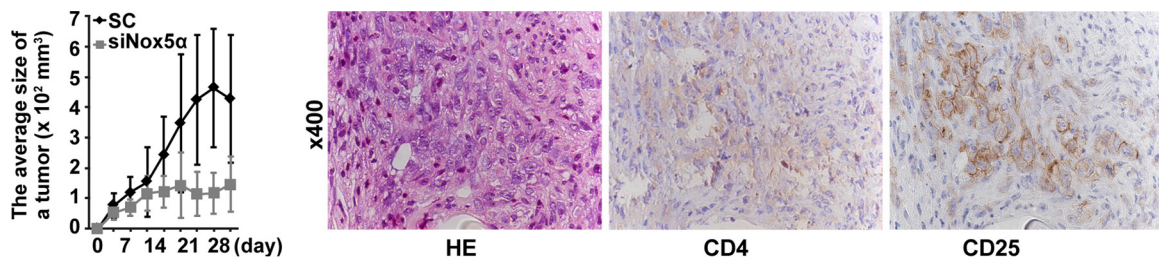In conclusion, our findings add a new dimension to the study

FIG 8 Tumor formation by Nox5α siRNA-transfected and control siRNA-transfected cell lines. MT2sc and MT2siNox5α cells were inoculated into NOG mice, and the growth rate of tumor was monitored by measuring tumor volumes over a 4-week period. The data represent means ± SD ($n = 6$). Student's t test was performed. $P > 0.05$ (versus scrambled data at 4 to 14 days; $P < 0.05$ (versus scrambled data at 17 to 28 days). Tumor samples were immunostained with anti-CD4 and anti-CD25 antibodies and counterstained with hematoxylin-eosin (HE).

of HTLV-1 neoplastic transformation by highlighting the tyrosine kinase-based regulation of Nox5α redox signaling and its pivotal role in the control of proliferation, survival, and motility of HTLV-1-transformed cells. Because deficiency of Nox5α-dependent ROS generation effectively suppresses the transformation phenotype of HTLV-1-infected cells, our discovery points to an intriguing possibility that Nox5α could be a potential molecular target for therapeutic intervention in cancer development.

REFERENCES

1. **Hinuma Y, Nagata K, Hanaoka M, Nakai M, Matsumoto T, Kinoshita KI, Shirakawa S, Miyoshi I.** 1981. Adult T-cell leukemia: antigen in an ATL cell line and detection of antibodies to the antigen in human sera. Proc Natl Acad Sci U S A **78:**6476–6480. http://dx.doi.org/10.1073/pnas.78.10.6476.

2. **Poiesz BJ, Ruscetti FW, Gazdar AF, Bunn PA, Minna JD, Gallo RC.** 1980. Detection and isolation of type C retrovirus particles from fresh and cultured lymphocytes of a patient with cutaneous T-cell lymphoma. Proc Natl Acad Sci U S A **77:**7415–7419. http://dx.doi.org/10.1073/pnas.77.12.7415.

3. **Miyoshi I, Kubonishi I, Yoshimoto S, Akagi T, Ohtsuki Y, Shiraishi Y, Nagata K, Hinuma Y.** 1981. Type C virus particles in a cord T-cell line derived by co-cultivating normal human cord leukocytes and human leukaemic T cells. Nature **294:**770–771. http://dx.doi.org/10.1038/294770a0.

4. **Popovic M, Lange-Wantzin G, Sarin PS, Mann D, Gallo RC.** 1983. Transformation of human umbilical cord blood T cells by human T-cell leukemia/lymphoma virus. Proc Natl Acad Sci U S A **80:**5402–5406. http://dx.doi.org/10.1073/pnas.80.17.5402.

5. **Grassmann R, Berchtold S, Radant I, Alt M, Fleckenstein B, Sodroski JG, Haseltine WA, Ramstedt U.** 1992. Role of human T-cell leukemia virus type 1 X region proteins in immortalization of primary human lymphocytes in culture. J Virol **66:**4570–4575.

6. **Yoshida M.** 2001. Multiple viral strategies of HTLV-1 for dysregulation of cell growth control. Annu Rev Immunol **19:**475–496. http://dx.doi.org/10.1146/annurev.immunol.19.1.475.

7. **Hall WW, Fujii M.** 2005. Deregulation of cell-signaling pathways in HTLV-1 infection. Oncogene **24:**5965–5975. http://dx.doi.org/10.1038/sj.onc.1208975.

8. **Mori N, Fujii M, Ikeda S, Yamada Y, Tomonaga M, Ballard DW, Yamamoto N.** 1999. Constitutive activation of NF-kappaB in primary adult T-cell leukemia cells. Blood **93:**2360–2368.

9. **Sun SC, Yamaoka S.** 2005. Activation of NF-kappaB by HTLV-I and implications for cell transformation. Oncogene **24:**5952–5964. http://dx.doi.org/10.1038/sj.onc.1208969.

10. **Leonard WJ, O'Shea JJ.** 1998. Jaks and STATs: biological implications. Annu Rev Immunol **16:**293–322. http://dx.doi.org/10.1146/annurev.immunol.16.1.293.

11. **Sun SC, Maggirwar SB, Harhaj EW, Uhlik M.** 1999. Binding of c-Rel to STAT5 target sequences in HTLV-I-transformed T cells. Oncogene **18:**1401–1409. http://dx.doi.org/10.1038/sj.onc.1202430.

12. **Migone TS, Lin JX, Cereseto A, Mulloy JC, O'Shea JJ, Franchini G, Leonard WJ.** 1995. Constitutively activated Jak-STAT pathway in T cells transformed with HTLV-I. Science **269:**79–81. http://dx.doi.org/10.1126/science.7604283.

13. **Xu X, Kang SH, Heidenreich O, Okerholm M, O'Shea JJ, Nerenberg MI.** 1995. Constitutive activation of different Jak tyrosine kinases in human T cell leukemia virus type 1 (HTLV-1) tax protein or virus-transformed cells. J Clin Invest **96:**1548–1555. http://dx.doi.org/10.1172/JCI118193.

14. **Lambeth JD.** 2007. Nox enzymes, ROS, and chronic disease: an example of antagonistic pleiotropy. Free Radic Biol Med **43:**332–347. http://dx.doi.org/10.1016/j.freeradbiomed.2007.03.027.

15. **Bedard K, Krause KH.** 2007. The NOX family of ROS-generating NADPH oxidases: physiology and pathophysiology. Physiol Rev **87:**245–313. http://dx.doi.org/10.1152/physrev.00044.2005.

16. **Kamata T.** 2009. Roles of Nox1 and other Nox isoforms in cancer development. Cancer Sci **100:**1382–1388. http://dx.doi.org/10.1111/j.1349-7006.2009.01207.x.

17. **Block K, Gorin Y.** 2012. Aiding and abetting roles of NOX oxidases in cellular transformation. Nat Rev Cancer **12:**627–637. http://dx.doi.org/10.1038/nrc3339.

18. **Bánfi B, Molnar G, Maturana A, Steger K, Hegedus B, Demaurex N, Krause KH.** 2001. A Ca(2+)-activated NADPH oxidase in testis, spleen, and lymph nodes. J Biol Chem **276:**37594–37601. http://dx.doi.org/10.1074/jbc.M103034200.

19. **Cheng G, Cao Z, Xu X, van Meir EG, Lambeth JD.** 2001. Homologs of gp91phox: cloning and tissue expression of Nox3, Nox4, and Nox5. Gene **269:**131–140. http://dx.doi.org/10.1016/S0378-1119(01)00449-8.

20. **Fu X, Beer DG, Behar J, Wands J, Lambeth D, Cao W.** 2006. cAMP-response element-binding protein mediates acid-induced NADPH oxidase NOX5-S expression in Barrett esophageal adenocarcinoma cells. J Biol Chem **281:**20368–20382. http://dx.doi.org/10.1074/jbc.M603353200.

21. **Sugamura K, Fujii M, Kannagi M, Sakitani M, Takeuchi M, Hinuma Y.** 1984. Cell surface phenotypes and expression of viral antigens of various human cell lines carrying human T-cell leukemia virus. Int J Cancer **34:**221–228. http://dx.doi.org/10.1002/ijc.2910340213.

22. **BelAiba RS, Djordjevic T, Petry A, Diemer K, Bonello S, Banfi B, Hess J, Pogrebniak A, Bickel C, Gorlach A.** 2007. NOX5 variants are functionally active in endothelial cells. Free Radic Biol Med **42:**446–459. http://dx.doi.org/10.1016/j.freeradbiomed.2006.10.054.

23. **Mitsushita J, Lambeth JD, Kamata T.** 2004. The superoxide-generating oxidase Nox1 is functionally required for Ras oncogene transformation. Cancer Res **64:**3580–3585. http://dx.doi.org/10.1158/0008-5472.CAN-03-3909.

24. **Komatsu D, Kato M, Nakayama J, Miyagawa S, Kamata T.** 2008. NADPH oxidase 1 plays a critical mediating role in oncogenic Ras-induced vascular endothelial growth factor expression. Oncogene **27:**4724–4732. http://dx.doi.org/10.1038/onc.2008.102.

25. **Dewan MZ, Terashima K, Taruishi M, Hasegawa H, Ito M, Tanaka Y, Mori N, Sata T, Koyanagi Y, Maeda M, Kubuki Y, Okayama A, Fujii M, Yamamoto N.** 2003. Rapid tumor formation of human T-cell leukemia virus type 1-infected cell lines in novel NOD-SCID/gammac(null) mice: suppression by an inhibitor against NF-kappaB. J Virol **77:**5286–5294. http://dx.doi.org/10.1128/JVI.77.9.5286-5294.2003.

26. **Janik P, Briand P, Hartmann NR.** 1975. The effect of estrone-progesterone treatment on cell proliferation kinetics of hormone-dependent GR mouse mammary tumors. Cancer Res **35:**3698–3704.

27. **Shi SR, Shi Y, Taylor CR.** 2011. Antigen retrieval immunohistochemistry: review and future prospects in research and diagnosis over two decades. J Histochem Cytochem **59:**13–32. http://dx.doi.org/10.1369/jhc.2010.957191.

28. **Sun SC, Ballard DW.** 1999. Persistent activation of NF-kappaB by the tax transforming protein of HTLV-1: hijacking cellular IkappaB kinases. Oncogene **18:**6948–6958. http://dx.doi.org/10.1038/sj.onc.1203220.

29. **Mulloy JC, Migone TS, Ross TM, Ton N, Green PL, Leonard WJ, Franchini G.** 1998. Human and simian T-cell leukemia viruses type 2 (HTLV-2 and STLV-2(pan-p)) transform T cells independently of Jak/STAT activation. J Virol **72:**4408–4412.

30. **Lin JX, Migone TS, Tsang M, Friedmann M, Weatherbee JA, Zhou L, Yamauchi A, Bloom ET, Mietz J, John S, Leonard WJ.** 1995. The role of shared receptor motifs and common Stat proteins in the generation of cytokine pleiotropy and redundancy by IL-2, IL-4, IL-7, IL-13, and IL-15. Immunity **2:**331–339. http://dx.doi.org/10.1016/1074-7613(95)90141-8.

31. **Shuai K, Halpern J, ten Hoeve J, Rao X, Sawyers CL.** 1996. Constitutive activation of STAT5 by the BCR-ABL oncogene in chronic myelogenous leukemia. Oncogene **13:**247–254.

32. **Burchill MA, Goetz CA, Prlic M, O'Neil JJ, Harmon IR, Bensinger SJ, Turka LA, Brennan P, Jameson SC, Farrar MA.** 2003. Distinct effects of

STAT5 activation on CD4+ and CD8+ T cell homeostasis: development of CD4+CD25+ regulatory T cells versus CD8+ memory T cells. J Immunol **171:**5853–5864. http://dx.doi.org/10.4049/jimmunol.171.11.5853.

33. **Ito M, Hiramatsu H, Kobayashi K, Suzue K, Kawahata M, Hioki K, Ueyama Y, Koyanagi Y, Sugamura K, Tsuji K, Heike T, Nakahata T.** 2002. NOD/SCID/gamma (c) (null) mouse: an excellent recipient mouse model for engraftment of human cells. Blood **100:**3175–3182. http://dx.doi.org/10.1182/blood-2001-12-0207.

34. **Takemoto S, Mulloy JC, Cereseto A, Migone TS, Patel BK, Matsuoka M, Yamaguchi K, Takatsuki K, Kamihira S, White JD, Leonard WJ, Waldmann T, Franchini G.** 1997. Proliferation of adult T cell leukemia/lymphoma cells is associated with the constitutive activation of JAK/STAT proteins. Proc Natl Acad Sci U S A **94:**13897–13902. http://dx.doi.org/10.1073/pnas.94.25.13897.

35. **Tomita M, Kawakami H, Uchihara JN, Okudaira T, Masuda M, Matsuda T, Tanaka Y, Ohshiro K, Mori N.** 2006. Inhibition of constitutively active Jak-Stat pathway suppresses cell growth of human T-cell leukemia virus type 1-infected T-cell lines and primary adult T-cell leukemia cells. Retrovirology **3:**22. http://dx.doi.org/10.1186/1742-4690-3-22.

36. **Bowman T, Garcia R, Turkson J, Jove R.** 2000. STATs in oncogenesis. Oncogene **19:**2474–2488. http://dx.doi.org/10.1038/sj.onc.1203527.

37. **Nicot C, Mulloy JC, Ferrari MG, Johnson JM, Fu K, Fukumoto R, Trovato R, Fullen J, Leonard WJ, Franchini G.** 2001. HTLV-1 p12(I) protein enhances STAT5 activation and decreases the interleukin-2 requirement for proliferation of primary human peripheral blood mononuclear cells. Blood **98:**823–829. http://dx.doi.org/10.1182/blood.V98.3.823.

38. **Kamiguti AS, Serrander L, Lin K, Harris RJ, Cawley JC, Allsup DJ, Slupsky JR, Krause KH, Zuzel M.** 2005. Expression and activity of NOX5 in the circulating malignant B cells of hairy cell leukemia. J Immunol **175:**8424–8430. http://dx.doi.org/10.4049/jimmunol.175.12.8424.

39. **Tagaya Y, Maeda Y, Mitsui A, Kondo N, Matsui H, Hamuro J, Brown N, Arai K, Yokota T, Wakasugi H.** 1989. ATL-derived factor (ADF), an IL-2 receptor/Tac inducer homologous to thioredoxin; possible involvement of dithiol-reduction in the IL-2 receptor induction. EMBO J **8:**757–764.

40. **Wakasugi N, Tagaya Y, Wakasugi H, Mitsui A, Maeda M, Yodoi J, Tursz T.** 1990. Adult T-cell leukemia-derived factor/thioredoxin, produced by both human T-lymphotropic virus type I- and Epstein-Barr virus-transformed lymphocytes, acts as an autocrine growth factor and synergizes with interleukin 1 and interleukin 2. Proc Natl Acad Sci U S A **87:**8282–8286. http://dx.doi.org/10.1073/pnas.87.21.8282.

41. **Mochizuki T, Furuta S, Mitsushita J, Shang WH, Ito M, Yokoo Y, Yamaura M, Ishizone S, Nakayama J, Konagai A, Hirose K, Kiyosawa K, Kamata T.** 2006. Inhibition of NADPH oxidase 4 activates apoptosis via the AKT/apoptosis signal-regulating kinase 1 pathway in pancreatic cancer PANC-1 cells. Oncogene **25:**3699–3707. http://dx.doi.org/10.1038/sj.onc.1209406.

42. **Silic-Benussi M, Cavallari I, Vajente N, Vidali S, Chieco-Bianchi L, Di Lisa F, Saggioro D, D'Agostino DM, Ciminale V.** 2010. Redox regulation of T-cell turnover by the p13 protein of human T-cell leukemia virus type 1: distinct effects in primary versus transformed cells. Blood **116:**54–62. http://dx.doi.org/10.1182/blood-2009-07-235861.